

Finite-Temperature Néel Ordering of Fluctuations in a Plaquette Orbital Model

Sandro Wenzel* and Wolfhard Janke†

Institut für Theoretische Physik and Centre for Theoretical Sciences (NTZ),
Universität Leipzig, Postfach 100 920, D-04009 Leipzig, Germany

(Dated: October 28, 2018)

We present a pseudo-spin model which should be experimentally accessible using solid-state devices and, being a variation on the compass model, adds to the toolbox for the protection of qubits in the area of quantum information. Using Monte Carlo methods, we find for both classical and quantum spins in two and three dimensions Ising type Néel ordering of energy fluctuations at finite temperatures without magnetic order. We also readdress the controversy concerning the stability of the ordered state in the presence of quenched impurities and present numerical results which are at clear variance with earlier claims in the literature.

PACS numbers: 02.70.Ss, 05.70.Fh, 75.10.Jm

I. INTRODUCTION

The prospect of topological quantum computation to implement fault tolerant quantum bits has led to considerable interest in the field¹ over the past years. A particular route within this area is the construction of simple (spin) models, as microscopic models of topological field theories, that allow a direct experimental realization. A hallmark is the so-called Kitaev model,² which is exactly solvable and known to be implementable as well as controllable using optical devices.³ Very recently, related efforts have been spent to construct similar models which can be realized using solid-state techniques.⁴ Guided by a few principles – a degenerate ground-state manifold and a gap to excited states – the so-called compass model (CM), with the Hamiltonian

$$\mathcal{H}_{\text{CM}} = J_x \sum_i S_i^x S_{i+e_x}^x + J_z \sum_i S_i^z S_{i+e_z}^z, \quad (1)$$

on an $L \times L$ lattice, was proposed as a simple model allowing for the protection of qubits.⁵ The CM is realizable by a particular arrangement of Josephson-junction devices and can be described by a Z_2 Chern-Simons topological quantum field theory.⁵ Extensions of (1) to global interactions possess even better fault tolerant properties.⁶

Originally introduced as an orbital model for Mott insulators,⁷ research into the actual CM has been pushed by several groups, which established degenerate ground-state properties,⁸ first-order quantum phase transitions,⁹ relation to $p + ip$ superconductivity,¹⁰ and the existence of directional order.^{11,12,13} Reference 12 argues that quantum spins support a resistivity of the ordered phase towards quenched disorder, which is in sharp contrast to classical degrees of freedom for which the ordered phase vanishes rapidly with increasing disorder. By a detailed Monte Carlo (MC) study¹³ of the quantum and classical CM, we have recently shown that this conclusion, however, needs further support as the CM shows unusual and extremely slowly converging finite-size scaling (FSS) properties on periodic lattices, which were used in Ref. 12. Recently, an interesting extension of (1) to include a magnetic field term hS was performed, leading to *thermal canting of spin order*.¹⁴

In the search for other fundamental spin models and to gain further insights into the field around the Kitaev model, we pro-

pose here a different – *geometric* – modification of the CM and concisely report on its intriguing physics. Our main result is the establishment of an interesting ordering that can be described by a crystallization and modulation of local energy contributions but which lacks conventional magnetic order. We show that the proposed model falls into the Ising universality class and that it possesses well behaved FSS properties in contrast to the CM. In the last part of this paper, we use this advantage to investigate the influence of (weak) quenched disorder in form of random vacancies to study their influence on the nature of the phase transition. We show that long-range order is completely lost already for very weak impurity concentrations.

II. THE MODEL

The plaquette orbital model (POM) is defined by the Hamiltonian

$$\mathcal{H}_{\text{POM}} = J_A \sum_{\langle i,j \rangle_A} S_i^x S_j^x + J_B \sum_{\langle i,j \rangle_B} S_i^z S_j^z, \quad (2)$$

where S^x and S^z are components of a two-component spin S , which can represent both classical and quantum degrees of freedom. In the latter case S^x and S^z are represented by the usual $S = 1/2$ Pauli matrices while in the classical case they denote projections of a continuous spin parameterized by an angle θ on the unit sphere. The bonds $\langle i, j \rangle_A$, $\langle i, j \rangle_B$ on sub-lattices A and B are arranged as depicted in Fig. 1. The coupling strengths J_A and J_B are in principle arbitrary. Here, we are interested in the isotropic case $J_A = J_B = J = 1$. The sign of J has no relevance since it can be transformed away on bipartite lattices.¹¹ With $N = L^d$ we denote the number of spins on a cubic lattice of linear extension L and dimension d . It should be emphasized that in contrast to the CM in three dimensions (3D) or the Kitaev model in two dimensions (2D), quantum MC investigations of the POM can easily be done also in 3D since there is no sign problem.

Note that the Hamiltonian (2) is Z_2 symmetric under exchange of sub-lattices A and B and spin indices x and z . Define further four-spin operators

$$P_r = S_r^z S_{r+e_x}^z S_{r+e_y}^z S_{r+e_x+e_y}^z \quad (3)$$

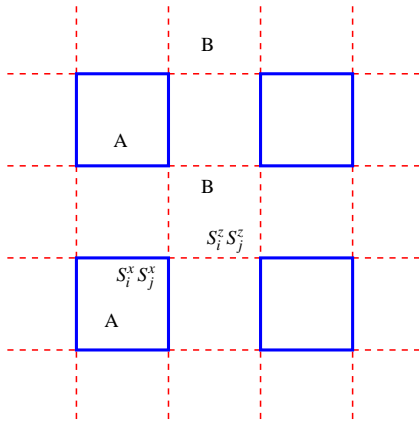


FIG. 1: (color online). Illustration of the POM lattice. The blue (thick) bonds indicate $S^x S^x$ terms while the red (dashed) bonds stand for $S^z S^z$ links. The lattice is closely related to a checkerboard. The generalization to the 3D POM is straightforward with sub-lattices A and B being cubes rather than plaquettes.

and

$$Q_l = S_l^x S_{l+e_x}^x S_{l+e_y}^x S_{l+e_y+e_x}^x, \quad (4)$$

with e_x and e_y being unit vectors on the lattice and r (l) a site pointing to the lower left corner of A (B) plaquettes. We can show that $[\mathcal{H}_{\text{POM}}, P_r] = [\mathcal{H}_{\text{POM}}, Q_l] = 0$ are local symmetries. Hence, on A plaquettes the operations $S_i^x \rightarrow -S_i^x, S_i^z \rightarrow S_i^z$ are symmetries with the analog expression on B plaquettes reading $S_i^x \rightarrow S_i^x, S_i^z \rightarrow -S_i^z$.⁸ For any r and $L > 2$, there further exists at least one index l such that $[P_r, Q_l] \neq 0$.¹⁵ This shows that every energy eigenvalue of \mathcal{H}_{POM} is at least two-fold degenerate. Performing an exact diagonalization employing invariant subspaces of the operator P (see Ref. 8), we could obtain all eigenvalues on a $N = 4 \times 4$ cluster confirming this conclusion. The POM hence possesses the same behavior as the CM in this regard. Whether the excitation gap persists in the infinite-volume limit remains to be investigated. The 3D extension of the model is obvious. Every plaquette becomes a cube, otherwise all arguments stay the same.

We now turn to a stochastic investigation of the model using established MC methods ranging from Metropolis sampling for classical variables to the quantum stochastic series expansion (SSE).^{16,17} Key to successfully simulate model (2) on large lattices is the use of parallel tempering methods to avoid barriers and reduce autocorrelation times. Details of our approach can be found in Ref. 13.

III. RESULTS

A. Néel ordering

The exchange symmetry ($A \Leftrightarrow B$) provides the possibility for spontaneous symmetry breaking. To see if this exchange symmetry is broken for some temperature $T < T_c$ a suitable

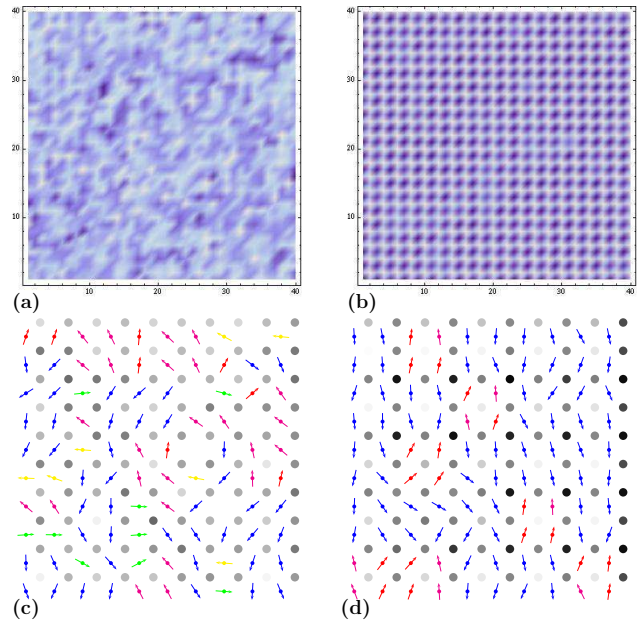


FIG. 2: (color online). Snapshots of the plaquette energy distribution on a $N = 40 \times 40$ lattice taken at $T = 1.0$ and $T = 0.02$, respectively. In the high-temperature regime (a) the system is disordered and a symmetry breaking has occurred in (b) for T less than a critical temperature T_c . Darker regions (color) represent lower energy. Figures (c) and (d) are snapshots of configurations in spin space corresponding to the high- and low-temperature phases for $L = 10$. No evident magnetic order is seen. The circles in (c) and (d) signify local energy density where darker means larger negative energy. Spins are color (gray) coded to make their direction more apparent.

order parameter should be defined. Let us just consider energy fluctuation on the two sub-lattices. Then, following Refs. 12, 13,18 we define the quantity

$$D = \frac{1}{N} |E_A - E_B|, \quad (5)$$

where $E_A = J_A \sum_{\langle i,j \rangle_A} S_i^x S_j^x$ is the energy contribution on sub-lattice A with the obvious relation for E_B . The suitability of that quantity can be seen in Fig. 2(a,b) which shows snapshots of the energy distribution at high and low temperatures. We can clearly observe a phase transition and the low-temperature phase can be described as a crystalline Néel state expressing up-down energy modulations. Further, this state is entirely described by energy fluctuations as there is no sign of long-ranged magnetic order seen in Fig. 2(c,d), as expected.¹¹ A quantity directly probing a crystalline state as in Fig. 2(b) is for example a plaquette structure factor defined by

$$S_{\text{pl}} = (1/N) \sum_r^N (-1)^{x_r+y_r} S_{\text{P}}(0) S_{\text{P}}(r), \quad (6)$$

where

$$S_{\text{P}}(r) = S_r S_{r+e_x} + S_{r+e_y} S_{r+e_x+e_y} + S_r S_{r+e_y} + S_{r+e_x} S_{r+e_x+e_y} \quad (7)$$

is a four-site spin operator on a plaquette. The sign of $(-1)^{x_r+y_r}$ alternates between A and B plaquettes. We will show below that S_{pl} is indeed an order parameter.

B. Monte Carlo simulations

Having visualized the onset of crystalline order, we now turn to a more careful discussion of the phase transition from comprehensive MC runs. Finite lattices are studied using two types of boundary conditions. In principle, we do not expect unwanted excitation as in the CM which spoil the FSS on periodic lattices,¹³ but we also study open boundary conditions to gain further confidence in our results. Open boundary conditions have the additional advantage that they prefer one sub-lattice over the other thus possibly stabilizing the ordered phase from the surface. In the latter case the $|\dots|$ in Eq. (5) can be also left away from the definition of the order parameter. In 2D, simulations were performed of both the classical and quantum cases for various lattice sizes $L = 10, \dots, 96$, which proved to be sufficiently large. Our analysis to obtain the critical temperatures is based on D , rather than S_{pl} because it is easier measured and is less susceptible to statistical noise. Detection of the phase boundary proceeds, as usual, by considering the susceptibility

$$\chi = N(\langle D^2 \rangle - \langle D \rangle^2), \quad (8)$$

or the Binder parameter defined as

$$B = 1 - \langle D^4 \rangle / (3\langle D^2 \rangle^2). \quad (9)$$

Figure 3(a) summarizes data obtained for the classical model for the order parameter D as well as the structure factor S_{pl} (in inset). Both quantities clearly numerically establish existence of crystalline order. In Fig. 3(b), data for B and the susceptibility χ (in inset) is given which suggests a second-order phase transition at $T_{\text{c;cl}} = 0.0855(4)$ from the crossings of the Binder parameter. The value of $B(T_{\text{c}}) = 0.610(5)$ at the critical temperature is consistent with the usual 2D Ising value on the torus topology.^{19,20} We further investigate the critical temperature by a FSS analysis of the maxima of the susceptibility χ . By fitting the corresponding data in Fig. 3(c) to the usual ansatz

$$T_{\text{max}}(L) = T_{\text{c}} + aL^{-1/\nu} + bL^{-w}, \quad (10)$$

we obtain $T_{\text{c;cl}} = 0.0860(2)$ and $T_{\text{c;qu}} = 0.048(1)$ for the classical and quantum cases, respectively. Here, we assume the 2D Ising exponent $\nu = \nu_{2\text{DIsing}} = 1$ (justified by the fit quality and independent fits to the slope of the Binder parameters), and the effective correction term $\sim L^{-w}$ is used only in fits for open boundary conditions. Since these critical values are consistently obtained for open and periodic boundary conditions, we arrive at the important conclusion that FSS in the POM is well behaved, in clear distinction to the CM. It is then instructive to compare those values with the related critical temperatures of the directional-ordering transition in the CM. In Ref. 13, we obtained $T_{\text{c;cl}} = 0.1464(2)$

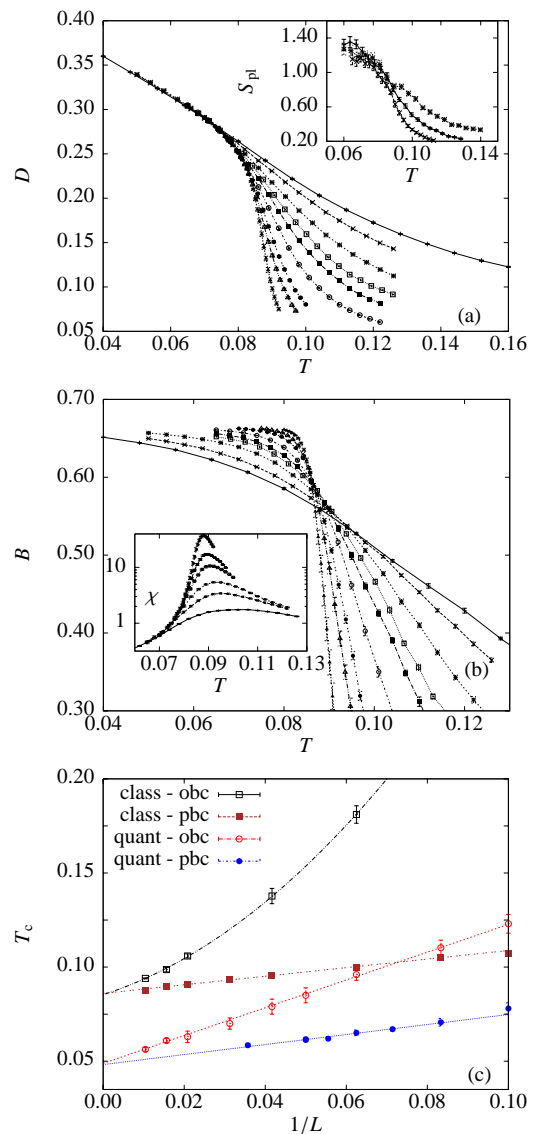


FIG. 3: (color online). Results from classical and quantum MC simulations for the 2D POM. (a) The order parameter D for various lattice sizes $L = 10$ to $L = 96$ for the classical model employing periodic boundary conditions. The inset shows the plaquette structure factor S_{pl} for $L = 20$, $L = 32$, and $L = 42$. The order parameter indicates a clear crystallization effect for $T < 0.086$. (b) The classical Binder parameter B close to the transition temperature supporting a second-order phase transition. The inset shows the susceptibility χ on a logarithmic scale for $L \geq 16$. Generally, steeper curves in (a) and (b) correspond to larger lattice sizes. (c) The critical temperatures T_{c} from FSS of the maxima locations of the susceptibility for both the classical and quantum cases and two different boundary conditions (open = obc, periodic = pbc).

and $T_{\text{c;qu}} = 0.055(1)$, which leads us to the conclusion that the geometric variation from Hamiltonian (1) to (2) results in a drastic reduction of T_{c} by 42% for classical fields vs only 13% for the quantum case.

In order to obtain further clarity on the type of the transition, we go one step further and study the model in three

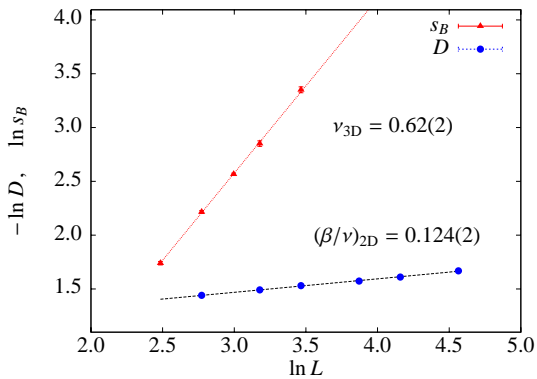


FIG. 4: (color online). FSS of the order parameter D for a 2D system and for the slope s_B of the Binder parameter for a 3D system. Both quantities are calculated at the critical temperatures and yield the expected Ising exponents.

dimensions for various lattice sizes $L = 8, \dots, 32$. Without showing details but by performing the same simulations and FSS analysis as before, we obtain a clear signal for a long-ranged *cube-ordered* state below the transition temperatures $T_{c;cl}^{3D} = 0.365(1)$ and $T_{c;qu}^{3D} = 0.180(5)$ for classical and quantum degrees of freedom, respectively. Interestingly, the increase in T_c (compared to the 2D transition temperatures) is larger for the classical model.

The proposition that the transition is of Ising type (as suggested by the symmetry and Binder parameter in Fig. 3(b)) should be reflected in the critical exponents. In Fig. 4 we select two quantities to address this question, namely the order parameter D for the 2D case and the slope s_B of the Binder parameter at the critical point for the 3D case. By performing fits to the ansatz $D \sim L^{-\beta/\nu}$ and $s_B \sim L^{1/\nu}$, we obtain in the classical cases $(\beta/\nu)_{2D} = 0.124(2)$ and $\nu_{3D} = 0.62(2)$, which are in excellent agreement with the theoretical value $(\beta/\nu)_{2D} = 1/8$ and high-precision literature²¹ on ν_{3D} . Figure 4 shows this scaling versus the lattice size of both observables at the critical temperatures in a log-log plot. The good quality of our data is apparent. This establishes that the transition in the POM has Ising exponents for both 2D and 3D, and – more importantly – that the *energetic* quantity D really scales like a (magnetic) order parameter. For the quantum case, this analysis is not so easy but our data is consistent with this conclusion.

C. Dilution effects in the POM

As the preceding analysis indicates that we have good FSS behavior in the present model, it is well suited to re-address the important question of impurity effects¹² in orbital models. To this end, we employ periodic boundary conditions and define a fraction x of quenched impurity sites, i.e., we remove each spin with probability x . Following Ref. 12, our objective is to study the quantity $g(x) = T_c(x)/T_c(0)$ to learn about the degree of stability of the Néel-ordered phase against dilution disturbances. With $T_c(x)$ one refers to the critical

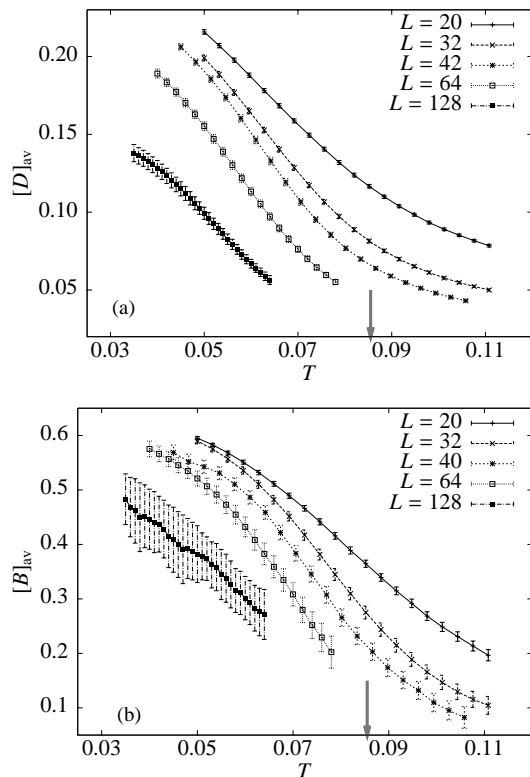


FIG. 5: Plot of (a) the disorder averaged (order) parameter $[D]_{av}$ and (b) the disorder averaged Binder ratio $[B]_{av}$ versus temperature T for $x = 1\%$ site dilution in the classical case. The Binder parameter does not show any signature of a remaining phase transition for sizes up to $L = 128$ and temperatures down to $T = 0.03$. The critical temperature in the clean case is indicated by the arrow.

temperature of the phase transition with dilution x . In order to access $T_c(x)$, we performed simulations on lattice sizes $L = 20, 32, 42, 64, 128$ (classical case) and $L = 20, 32$ (quantum case), where we generated and studied 100 – 200 different disorder realizations, respectively. The quantities $[D]_{av}$, $[\chi]_{av}$, and $[B]_{av}$ denote the disorder averaged values of the respective quantities defined above.

Studying just the (peaks of the) averaged susceptibility or the order parameter on moderate lattices sizes ($L = 20, 32, 42$), one could deduce values for $g(x)$ which are of the order of $g(x) \approx 0.70$ for the classical case vs $g(x) \approx 0.82$ for the quantum model in case of weak impurity concentration with $x = 0.01$. These values seem to be in qualitative agreement with earlier claims and in support of the conclusion of Ref. 12 that quantum fluctuations make the ordered phase more robust.

However, our simulations on bigger lattices for $x = 0.01$ reveal that the transition is, in fact, vanishing in the thermodynamic limit, implying $g(x) = 0, \forall x > 0$. This conclusion can be drawn for example from the data shown in Fig. 5. While the order-parameter $[D]_{av}$ seems to indicate some crossover which gets weaker for larger L , the Binder parameter $[B]_{av}$ clearly shows no crossing, i.e., no sign of critical behavior.

Remarkably, quite large lattice sizes $L \approx 128$ are needed to see this. These data obviously rule out the presence of a true phase transition in the vacancy diluted classical POM.

This situation is further reminiscent of the ordinary 2D Ising model subjected to a random field (at a fraction x of the sites) which is known not to exhibit a finite-temperature phase transition from theoretical²² and numerical works²³. While in the Ising model the random field destroys the Z_2 up-down spin symmetry, dilution in the POM breaks the $A - B$ plaquette symmetry. Such *random* local symmetry breaking is also known to destroy long-range order in, e.g., 2D antiferromagnetic Ising models with nearest and next-nearest neighbor interactions.²⁴

By the same argument it is clear that there is no phase transition in the 2D classical CM at any finite dilution x and the statements and conclusions of Ref. 12 are therefore at variance with the findings in this work. We also see no argument why the quantum CM should behave differently in this respect and suspect that quantum effects merely increase the stability of the low-temperature state on *finite and small* clusters of spins — an observation that might still be useful for applications.

IV. CONCLUSION

We have introduced and investigated a plaquette orbital model related to the Kitaev model and the CM. The present

work establishes that this model exhibits an unconventional finite-temperature phase transition from a disordered to a Néel-ordered state in the energy distribution. It thus displays antiferromagnetic features without possessing magnetic order. By symmetry arguments and MC simulations, the critical exponents were determined to be in the Ising universality class. The geometric variation from the CM to the plaquette orbital model results in a substantial lowering of the ordering temperature for the classical model, which is not the case for quantum spins. Our subsequent analysis of the POM in the presence of impurities shows that long-range ordering is lost for (any) weak disorder concentration. This finding also sheds concluding light on the somewhat controversial issue concerning the effect of impurities on the ordered phase in the compass model.^{12,13} A more detailed analysis of the nature of the ground states for arbitrary J_A, J_B and its quantum phase transitions^{9,25} would be an interesting continuation of this work as would be a thorough investigation of the excitations in the POM. Apart from its possible relevance for protected qubits, the present model should also be of immediate interest for the physics of orbital models in relation to transition-metal oxides.²⁶

We thank V. W. Scarola, B. Douçot, A. Läuchli, and T. Vojta for discussions. Work supported by the Studienstiftung des deutschen Volkes, the Deutsch-Französische Hochschule (DFH), the DFG graduate school “BuildMoNa,” and NIC Jülich.

* Present address: Max-Planck-Institute for Physics of Complex Systems, Nöthnitzer Str. 38, 01187 Dresden, Germany; Electronic address: wenzel@itp.uni-leipzig.de

† Electronic address: janke@itp.uni-leipzig.de

¹ A. Y. Kitaev, *Ann. Phys.* **303**, 2 (2003).

² A. Y. Kitaev, *Ann. Phys.* **321**, 2 (2006).

³ L. M. Duan, E. Demler, and M. D. Lukin, *Phys. Rev. Lett.* **91**, 090402 (2003); A. Micheli, G. K. Brennen, and P. Zoller, *Nat. Phys.* **2**, 341 (2006); C. Zhang, V. W. Scarola, S. Tewari, and S. D. Sarma, *Proc. Nat. Acad. Sci. USA* **104**, 18415 (2007); S. Dusuel, K. P. Schmidt, and J. Vidal, *Phys. Rev. Lett.* **100**, 177204 (2008); L. Jiang, G. K. Brennen, A. V. Gorshkov, K. Hammerer, M. Hafezi, E. Demler, M. D. Lukin, and P. Zoller, *Nat. Phys.* **4**, 482 (2008).

⁴ S. Gladchenko, D. Olaya, E. Dupont-Ferrier, B. Douçot, L. B. Ioffe, and M. E. Gershenson, *Nat. Phys.* **5**, 48 (2008); G. Jackeli and G. Khaliullin, *Phys. Rev. Lett.* **102**, 017205 (2009).

⁵ B. Douçot, M. V. Feigel'man, L. B. Ioffe, and A. S. Ioselevich, *Phys. Rev. B* **71**, 024505 (2005).

⁶ P. Milman, W. Mainault, S. Guibal, L. Guidoni, B. Douçot, L. Ioffe, and T. Coudreau, *Phys. Rev. Lett.* **99**, 020503 (2007).

⁷ K. Kugel and D. Khomskii, *Sov. Phys. Usp.* **25**, 231 (1982).

⁸ J. Dorier, F. Becca, and F. Mila, *Phys. Rev. B* **72**, 024448 (2005).

⁹ H.-D. Chen, C. Fang, J. Hu, and H. Yao, *Phys. Rev. B* **75**, 144401 (2007); R. Orús, A. C. Doherty, and G. Vidal, *Phys. Rev. Lett.* **102**, 077203 (2009).

¹⁰ Z. Nussinov and E. Fradkin, *Phys. Rev. B* **71**, 195120 (2005).

¹¹ A. Mishra, M. Ma, F.-C. Zhang, S. Guertler, L.-H. Tang, and S. Wan, *Phys. Rev. Lett.* **93**, 207201 (2004).

¹² T. Tanaka and S. Ishihara, *Phys. Rev. Lett.* **98**, 256402 (2007).

¹³ S. Wenzel and W. Janke, *Phys. Rev. B* **78**, 064402 (2008).

¹⁴ V. W. Scarola, K. B. Whaley, and M. Troyer, *Phys. Rev. B* **79**, 085113 (2009).

¹⁵ For $L = 2$ and periodic boundary conditions this is not the case as (2) is equivalent to the normal XY model.

¹⁶ A. W. Sandvik, *Phys. Rev. B* **59**, R14157 (1999).

¹⁷ O. F. Syljuåsen and A. W. Sandvik, *Phys. Rev. E* **66**, 046701 (2002).

¹⁸ C. D. Batista and Z. Nussinov, *Phys. Rev. B* **72**, 045137 (2005).

¹⁹ J. Salas and A. D. Sokal, *J. Stat. Phys.* **98**, 551 (2000).

²⁰ W. Selke, *Eur. Phys. J. B* **51**, 223 (2006).

²¹ A. Pelissetto and E. Vicari, *Phys. Rep.* **368**, 549 (2002).

²² See, e.g., G. Grinstein and S. Ma, *Phys. Rev. Lett.* **49**, 685 (1982); T. Nattermann, *J. Phys. C* **16**, 6407 (1983).

²³ See, e.g., I. B. Ferreira, A. R. King, V. Jaccarino, J. L. Cardy, and H. J. Guggenheim, *Phys. Rev. B* **28**, 5192 (1983); J. F. Fernandez and E. Pytte, *Phys. Rev. B* **31**, 2886 (1985).

²⁴ J. F. Fernández, *Phys. Rev. B* **38**, 6901 (1988); A. Aharony, *Phys. Rev. B* **44**, 423 (1991).

²⁵ M. Vojta, *Rep. Prog. Phys.* **66**, 2069 (2003).

²⁶ See, e.g., Y. Tokura and N. Nagaosa, *Science* **288**, 462 (2000); Z. Nussinov, M. Biskup, L. Chayes, and J. van den Brink, *Europhys. Lett.* **67**, 990 (2004).